Dexmedetomidine attenuates neuronal injury induced by cerebral ischemia-reperfusion by regulating miR-199a

YULIN ZHU[1], HUATANG ZHAO[2], WENSHAN ZHANG[3], XINGANG MA[4] and YE LIU[4]

[1]Department of Anesthesiology, Yantaishan Hospital, Yantai, Shandong 264000; [2]Department of Anesthesiology, The Second Hospital of Liaocheng Affiliated to Shan-dong First Medical University, Liaocheng, Shandong 252000; [3]Department of Anesthesiology, Laixi People's Hospital, Qingdao, Shandong 266600; [4]Department of Anesthesiology, Zibo Maternal and Child Health Hospital, Zibo, Shandong 255000, P.R. China

Received November 25, 2020; Accepted April 21, 2021

DOI: 10.3892/mmr.2021.12213

Abstract. As is well known, dexmedetomidine (DEX) serves a neuroprotective role in cerebral ischemia-reperfusion (CIR) injury, and microRNA (miR)-199a has been re-ported to be associated with IR injury. However, the association between DEX and miR-199a in CIR injury remains unknown. Thus, the aim of the present study was to verify whether the neuroprotective effect of DEX on cerebral ischemia-reperfusion rats is associated with miR-199a. A rat model of CIR was established, and the modified neurological severity score (mNSS) was evaluated. The effect of DEX on the patholog-ical structure of the cerebral cortex in CIR rats was observed by hematoxylin and eosin and Nissl staining. Reverse transcription-quantitative PCR was used to analyze the expression levels of miR-199a in brain tissue following intracerebroventricular injection of miR-199a antagomir. The co-expression of NeuN and microtubule-associated proteins 1A/1B light chain 3B in the cerebral cortex was analyzed by immunofluorescence staining. Western blotting and immunohistochemistry were performed to analyze the expression of autophagy-associated proteins in the brain tissue. DEX inhibited the expression of miR-199a, decreased the mNSS and improved pathological damage to the cerebral cortex. DEX also inhibited autophagy and expression levels of associated proteins and decreased nerve cell injury. In conclusion, DEX inhibited expression of miR-199a and improved neurocyte injury induced by CIR.

Introduction

Stroke is the second leading cause of mortality worldwide, with an annual mortality of ~5.5 million, and causes disability in 50% of survivors (1). Ischemic stroke accounts for 75-85% of all strokes and is a pathological state characterized by limited blood flow (2). With regards to hindered cerebral blood supply, the most common clinical treatment for ischemic stroke is restoration of perfusion and reoxygenation to the affected area (3). However, reoxygenation and blood flow recovery are associated with aggravation of tissue injury and a severe inflammatory response, which is known as cerebral ischemia-reperfusion (CIR) injury (4,5). Due to the complex mechanism of cerebral ischemia, clinical treatment is difficult. Therefore, it is urgent to find effective treatment for cerebral ischemia.

Dexmedetomidine (DEX) is a novel type of analgesic (6). Multiple studies have shown that DEX exerts its role via anti-inflammatory and anti-apoptotic pathways, and it is used in the treatment of neuropathic pain and other diseases (7-9). However, the mechanism of the protective effect of DEX is still unclear. Certain studies have shown that DEX serves a neuroprotective role by inhibiting endoplasmic reticulum stress (10,11). The present study investigated whether DEX inhibits expression of microRNA (miRNA/miR)-199a and improves neurocyte injury induced by CIR injury.

Previously, non-coding RNA has attracted significant attention (12-15). Non-coding RNAs comprise ribosomal, transfer, small nuclear and long non-coding RNA, as well as miRNA. miRNAs are endogenous short single-stranded RNAs (12). Previ-ous studies have investigated the role of miRNAs in cancer, particularly the potential of miRNAs as specific biomarkers of cancer (13,14). In addition to cancer, miRNA serves an important role in regulation of gene expression in various biological pathophysiological processes (15). In the central nervous system, pathological conditions, including stroke, schizophrenia and neurodegenerative disease, significantly alter expression of miRNAs in the brain and affect the occurrence of disease (16,17). miRNAs have been reported to be associated with IR injury, including miR-455 and miR-199a. Furthermore, miR-199a has been shown to recognize and target sirtuin 1, thereby repressing hypoxia preconditioning and longevity of cardiac myocytes (18-20). Therefore, it was hypothesized that DEX may serve a role in CIR injury by targeting miR-199a.

In the present study it was hypothesized that the neuroprotection of DEX may be associated with miR-199a in CIR

Correspondence to: Dr Ye Liu, Department of Anesthesiology, Zibo Maternal and Child Health Hospital, 66 North Tianjin Road, Zhangdian, Zibo, Shandong 255000, P.R. China
E-mail: ly18853385283@126.com

Key words: dexmedetomidine, cerebral ischemia-reperfusion, microRNA-199a, autophagy

injury. Thus, the miR-199a antagomir was used to determine the mechanism of DEX in a rat model of CIR injury.

Materials and methods

Animals. In total, 72 healthy SPF grade Sprague Dawley male rats (weight, 180-220 g; age, 6-8 weeks) were purchased from Jinan Pengyue Experimental Animal Co., Ltd. [licence no. SCXK (Lu) 20190003]. All rats were housed under controlled temperature (22±2˚C) and humidity (55±5%), with free access to food and water, and were subjected to adaptive feeding for 1 week under a 12-h light/dark cycle. Animal experiments were performed in accordance with the Guide for the Care and Use of Laboratory Animals, 8th edition (21) and were approved by the Animal Protection and Use Committee of Yantaishan Hospital (Yantai, China).

CIR model. Before the operation, rats were fasted for 12 h and allowed to drink water; the percentage of maximum body weight loss was 0.10%. According to the Zea Longa method (22), the CIR model was established using middle cerebral artery occlusion. Rats were anesthetized via intraperitoneal injection of sodium pentobarbital (50 mg/kg) and fixed in a supine position. The common, internal and external carotid arteries were carefully separated along the midline of the neck. Next, a nylon thread was inserted into the internal carotid artery. Upon feeling slight resistance, the insertion of the nylon thread was halted and fixed in place. After blocking blood flow for 2 h, the thread was removed, and reperfusion was permitted for 24 h. The wound was sutured layer-by-layer after the operation. During the operation, the room temperature was maintained at 37.0±0.5˚C, and the rectal temperature, respiratory rate and heart rate of animals were monitored. After animals woke up, gait and behavior were observed, and the success of modeling was judged according to the following scoring standard, as previously described (8,22,23): Grade 0 (normal), symptoms without neurological impairment; grade 1 (mild), inextensibility of the left forepaw when lifting the rat tail; grade 2 (moderate), circling to the left side while walking; grade 3 (severe), walking difficulty and leaning to the left; grade 4 (very severe), inability to walk spontaneously. Rats with a score of 1-3 were selected for subsequent experiments. The thread in rats in the sham operation group was removed immediately after inserting the thread plug without retaining the middle cerebral artery.

Intracerebroventricular injection. Following routine anesthesia using sodium pentobar-bital (50 mg/kg), the rats were fixed on a stable stereotactic instrument. After skin preparation and disinfection using 2.5% iodine, the top skin of the head was cut (depth, 1-2 cm), and the anterior fontanel was exposed. Head fixation of rats was as follows: The nose was in the middle of the fixator; front and rear fontanelle were kept at the same level; and the head was firmly fixed. The diameter of the drill hole was ~0.5 mm, and the bregma coordinates were as follows: AP, 0.8 mm; L, 1.5 mm; and V, 4.5 mm, based on the rat brain stereotaxic atlas (24). The miR-199a antagomir or negative con-trol was slowly injected into the lateral ventricle at an injection rate of 0.5 μl/min using a microinjector. Then, the needle was slowly removed and the small hole was sealed with medical bone wax. The incision was sutured following local routine disinfection.

Animal grouping and treatment. The animals were randomly divided into the following groups: i) Sham; ii) CIR model; iii) DEX; iv) miR-199a antagomir (anta-miR); v) anta-miR + negative control (NC); and vi) DEX + anta-miR (n=12/group). In the Sham group, the thread was removed immediately after inserting the thread plug, without retaining the middle cerebral artery and rats were fed normally. In the CIR model group, CIR injury was induced. In the DEX group, 3 μg/kg/h DEX was injected into the caudal vein 24 h before the operation and during reperfusion, as previously described (8). At 0.5 h before reperfusion, animals in the anta-miR group were injected with 5 μl anta-miR (Shanghai GenaPharma Co., Ltd.; https://www.genepharma.com/en/) in the breg-ma coordinates AP, 0.8 mm; L, 1.5 mm; and V, 4.5 mm (based on the rat brain stereo-taxic atlas). In the NC antagomir group (anta-NC), 0.5 h before perfusion, 5 μl anta-miR NC (5'-UAACCAAUGUGCAGACUACUGU-3'; Shanghai GenaPharma Co., Ltd.), was injected into the right ventricle at the aforementioned coordinates. In the DEX + anta-miR group, DEX was administered twice: 3 μg/kg/h DEX was injected into the tail vein 24 h before the operation and at the beginning of reperfusion, separately. In addition, 5 h before reperfusion, 5 μl anta-miR was injected into the right ventricle of rats (bregma coordinates: AP, 0.8 mm; L, 1.5 mm; and V, 4.5 mm, based on the Rat Brain Stereotaxic Atlas). Following 24 h reperfusion, the rats were anesthetized with 3% pentobarbital sodium (45 mg/kg), followed by euthanasia via cervical dislocation.

The brain tissue of 6 rats in each group was fixed in 4% paraformaldehyde at 37˚C for 24 h for 2,3,5-triphenyltetrazolium chloride (TTC) and hematoxylin and eosin (H&E) staining, immunofluorescence and immunohistochemistry. Brain tissue from another 6 rats in each group was stored in liquid nitrogen for western blotting and reverse transcription-quantitative PCR (RT-qPCR) analysis.

Improved mNSS. The neurobehavioral score of the experimental groups was assessed in a blinded manner. The neurological function of rats was evaluated before modeling and at 6, 12 and 24 h after reperfusion. The mNSS behavioral score is primarily used to assess ability, such as movement, sensation, balance and reflex, of rats (25). The score ranges from 0 to 18. The scoring criteria is showed in Table I. The higher the score, the more serious the neurological deficit. A total of 8 rats in each group were randomly selected for mNSS behavioral tests at 1, 3 and 7 days after the operation. The maximum score was 18 points, with 1-6 points allocated for mild, 7-12 for moderate and 13-18 for severe damage.

TTC staining. The volume of cerebral infarction was measured by TTC staining. Briefly, 5-μm coronal slices were cut and soaked in 2% TTC dye solution (cat. no. D025-1-3; Nanjing Jiancheng Bioengineering Institute) and incubated at 37˚C for 30 min. The slides were washed with ddH_2O and then stained by 2% TTC at 37˚C for 30 min. Finally, slides were fixed with 4% paraformaldehyde at 37˚C for 24 h, imaged with a camera (DSC-RX100M6; Sony Corporation)and processed with ImageJ software 5.0 (National Institutes of Health).

RT-qPCR. Animal tissue total RNA extraction kit (cat. no. N066; Nanjing Jiancheng Bioengineering Institute)

Table I. Modified neurological severity score (maximum points=18).

Test	Points
Raising rat by tail	3
Flexion of forelimb	1
Flexion of hindlimb	1
Head moves >10˚ to vertical axis within 30 sec	1
Placing rat on floor	3
Normal walk	0
Inability to walk straight	1
Circling toward the paretic side	2
Fall down to the paretic side	3
Sensory	2
Placing (visual and tactile)	1
Proprioceptive (deep sensation, pushing paw against table edge to stimulate limb muscles)	1
Beam balance	6
Balances with steady posture	0
Grasps side of beam	1
Hugs beam; one limb falls from beam	2
Hugs beam; two limbs fall from beam or spins on beam (>60 sec)	3
Attempts to balance on beam but falls off (>40 sec)	4
Attempts to balance on beam but falls off (>20 sec)	5
Falls off; no attempt to balance or hang on to beam (20 sec)	6
Reflex absence and abnormal movement	4
Pinna (head shake when auditory meatus is touched)	1
Corneal (eye blink when cornea is lightly touched with cotton)	1
Startle (motor response to brief snapping clipboard noise)	1
Seizure, myoclonus, myodystony	1

was used to extract total RNA from cortical tissue, according to the manufacturer's protocol, and agarose gel electrophoresis was used to detect the RNA integrity. A PrimeScript™ RT kit (cat. no. K1622; Thermo Fisher Scientific, Inc.) was used to reverse transcribe total RNA into cDNA at 37˚C according to the manufacturer's protocol. RT-qPCR was performed using SYBR Green PCR Master mix on an ABI 7300 Real Time PCR system (both Applied Biosystems; Thermo Fisher Scientific, Inc.). Primer 5.0 (Premier Biosoft International) was used to design RT-qPCR primers as follows: miR-199a forward (F), 5'-AGAAGGCGATTGATACGAGTCA-3' and reverse (R), 5'-GGTCTCCCCAGTGTTCAGATA-3'; and U6 F,5'-GTGCAGGGTCCGAGGT-3'andR,5'-CGCTTCGGCAG CACAT-3'. The thermocycling conditions used for RT-qPCR were as follows: Denaturation at 95˚C for 20 sec; followed by 40 cycles of annealing at 60˚C for 30 sec and extension at 72˚C for 30 sec. The melting curve was drawn and relative expression of miR-199a was analyzed by the $2^{-\Delta\Delta Cq}$ method (26).

H&E staining. The brain tissue was fixed in 4% paraformaldehyde at 37˚C for 24 h, dehydrated and embedded in paraffin. The sections were cut into 4-μm thick slices (three slices/group). The slices were placed into an oven at 60˚C for 12 h. Next, the slices were immersed in xylene I and II for 15 min; 100% ethanol I and II for 10 min; 95, 90, 80 and 70% gradient ethanol for 5 min; and ddH_2O for 5 min to remove residual ethanol. The slices were then stained with 0.3% hematoxylin for 5 min, and then stained blue with ddH_2O for 4 min at 37˚C. Next, the sections were briefly immersed in 1% hydrochloric acid-ethanol, washed and observed under an optical light microscope (BX51; Olympus Corporation) at x400 magnification until differentiation was moderately completed. The slices were then immersed in 0.5% eosin for 10 min at 37˚C, and the residual eosin was rapidly rinsed off using ddH_2O. Next, the slices were immersed in a 70, 80, 90, 95, 100 I and 100% II ethanol gradient series for dehydration for 5 min each and washed with xylene. Finally, the slices were sealed with neutral resin, and observed and photographed under an optical light microscope (BX51; Olympus Corporation) at x400 magnification.

Nissl staining. Staining was performed in accordance with the instructions of the Nissl staining kit (cat. no. BB44357-1; BestBio Science; http://www.bestbio.com.cn/). A 6-μm thick paraffin-embedded section was dewaxed using xylene and hydrated using gradient ethanol, washed with ddH_2O, stained with 0.5% methylene blue for 10 min at 37˚C and Nissl differentiated for 10 min at 37˚C. Under an optical light microscope, Nissl bodies were observed at x400 magnification. Next, the slices were treated with 0.5% ammonium molybdate solution for 5 min at 37˚C, washed with distilled water to prevent decolorization, dehydrated with anhydrous ethanol and then sealed with neutral

glue after being made transparent with xylene. The morphology of cortical neurons was observed under a light microscope (cat. no. BX51; Olympus Corporation) at x400 magnification.

Immunofluorescence. After being fixed with 4% paraformaldehyde at 37˚C for 24 h, brain tissue was embedded in paraffin and sectioned at a thickness of 4 μm. The slices were incubated at 50˚C for 1 h and then washed with PBS. Next, blocking at 37˚C was performed by addition of 10% goat serum (cat. no. 16210064; Gibco; Thermo Fisher Scientific, Inc.) for 1 h, followed by addition of mouse monoclonal antibody against rat NeuN (1:1,000; cat. no. ab104224; Abcam) and rabbit anti-rat microtubule-associated proteins 1A/1B light chain 3B (LC3B) polyclonal antibody (1:100; cat. no. ab222776; Abcam) overnight at 4˚C. Next, fluorescently labeled secondary antibody (FITC-labeled goat anti mouse IgG; 1:1,000; cat. no. ab678; Abcam) and Cy3-labeled goat anti-rabbit IgG (1:500; cat. no. ab6939; Abcam) were incubated with the membrane at room tem-perature for 1 h. DAPI staining (5 μg/ml) was conducted for 5 min at 25˚C, followed by fluorescence quenching agent sealing, fluorescence microscope observation with the magnification of x400 and imaging.

Immunohistochemistry. Paraffin-embedded sections (thickness, 5 μm) of brain tissue were incubated in an oven at 60˚C overnight and dewaxed in water. The antigen activity was restored by the high-pressure repair method, and 3% endogenous peroxidase ac-tivity was inactivated by H_2O_2 solution, followed by blocking with 10% goat serum (cat. no. 16210064; Gibco; Thermo Fisher Scientific, Inc.) at room temperature for 60 min. Next, rabbit anti-rat Beclin1 (1:500; cat. no. ab62557; Abcam), p62 (1:400; cat. no. ab91526; Abcam) and LC3B (1:2,000; cat. no. ab51520; Abcam) monoclonal antibod-ies were added at 4˚C for overnight. The NC group was incubated at 4˚C overnight with PBS instead of primary antibody. After rewarming at room temperature every oth-er day, horseradish peroxidase (HRP)-conjugated goat anti-rabbit IgG H&L secondary antibody was added (1:5,000; cat. no. ab205718; Abcam) at 37˚C for 10-15 min. Following 0.05% DAB staining at room temperature for 5 min, the sections were stained with hematoxylin at room temperature for 5 min. Following differentiation, the sections were dehydrated with 70% alcohol, 80% alcohol, 90% alcohol and 100% alcohol, made transparent and sealed. Sections were finally imaged under an optical light microscope (BX51; Olympus Corporation) at x400 magnification. The pathological images were collected and analyzed by Motic Medical 6.0 software [Motic (Xiamen) Electric Group Co., Ltd.]. A total of five non-overlapping visual fields were observed in each section. The number of Beclin1, p62 and LC3B-positive cells was counted, and the average value was calculated. Cells with brown cytoplasm (observed under light microscopy at x400 magnification) were regarded as positive.

Western blotting. The protein expression levels of Beclin1, p62, LC3B and cleaved caspase-3 in rat cerebral cortex were detected by western blotting. The cerebral cortex tissue was removed from liquid nitrogen and placed into a precooling mortar for 15 min. Protein lysate was added to the mortar to wash the ground tissue. After mixing, the suspension was placed into an Eppendorf tube. The suspension was placed on ice for 20 min and centrifuged at 850 x g for 20 min at 4˚C before the supernatant was collected. The total protein of each sample was detected by a BCA protein quantification kit. The supernatant was incubated with denatured 4X loading buffer solution (with DTT; cat. no. P1015; Beijing Solarbio Science & Technology Co., Ltd.) at a ratio of 3:1 and placed in a water bath at 100˚C for 10 min. Equal quantities of protein samples (30 μg) were separated by 10% SDS-PAGE and transferred to a PVDF membrane. The PVDF membrane was blocked with 5% skimmed milk powder at 4˚C for 60 min and incubated with rabbit anti-rat Beclin1 (1:1,000; cat. no. ab189494; Abcam), p62 (cat. no. ab52875; Abcam), cleaved caspase-3 (1:500; cat. no. ab49822; Abcam), LC3B (1:200; cat. no. ab222776; Abcam) and β-actin (1:1,000; cat. no. ab8277; Abcam) polyclonal antibodies at 4˚C overnight. After washing the membrane with washing solution, goat anti-rabbit IgG H&L (HRP) secondary antibody (1:5,000; cat. no. ab205718; Abcam) was added and incubated for 1 h at room temperature in the dark. Next, the exposure solution was prepared according to the manufacturer's instructions of the enhanced chemiluminescence kit (Thermo Fisher Scientific, Inc.), and the color rendering expo-sure was added to the PVDF film. ImageJ software 5.0 (National Institutes of Health) was used for quantitative analysis.

Statistical analysis. The data were analyzed with GraphPad Prism 5.0 statistical analysis software (GraphPad Software, Inc.), and three experimental repeats were performed and the results were expressed as the mean ± SD. One-way ANOVA was used, followed by Tukey's post hoc test, for comparisons between groups. $P<0.05$ was consid-ered to indicate a statistically significant difference.

Results

DEX improves CIR injury in rats by inhibiting miR-199a. Compared with the Sham group, the mNSS of the CIR group was significantly higher at 6 h after injury, at which point neurological deficit was greatest (Fig. 1A). At 12 and 24 h after injury, mNSS decreased and neurological function recovered. mNSS of the DEX and anta-miR groups were significantly lower than those of the CIR group across all three time points, and mNSS significantly decreased with time. Compared with the rats in the DEX and anta-miR groups, the scores of the DEX + anta-miR group were significantly decreased but did not reach the level of the Sham group. Fig. 1B shows slices of one rat brain from each group. There was no cerebral infarction in the Sham group. Compared with the Sham group, the area of cerebral infarction in the CIR and anta-NC groups was significantly increased. Following DEX and anta-miR treatment, the cerebral infarction area significantly decreased. Compared with the DEX or anta-miR groups, the infarct area was further decreased in DEX + anta-miR group. miR-199a was weakly expressed in the cortex of rats with CIR. DEX and anta-miR pretreatment decreased the content of miR-199a, and the content of miR-199a was further decreased in DEX + anta-miR group (Fig. 1C). These data revealed that the neuroprotection of DEX was associated with miR-199a.

Effect of DEX on cerebral cortex pathology in rats with CIR. The nucleoli of neurons in the cortex of the Sham group were clear and the neurons exhibited normal morphology (Fig. 2A).

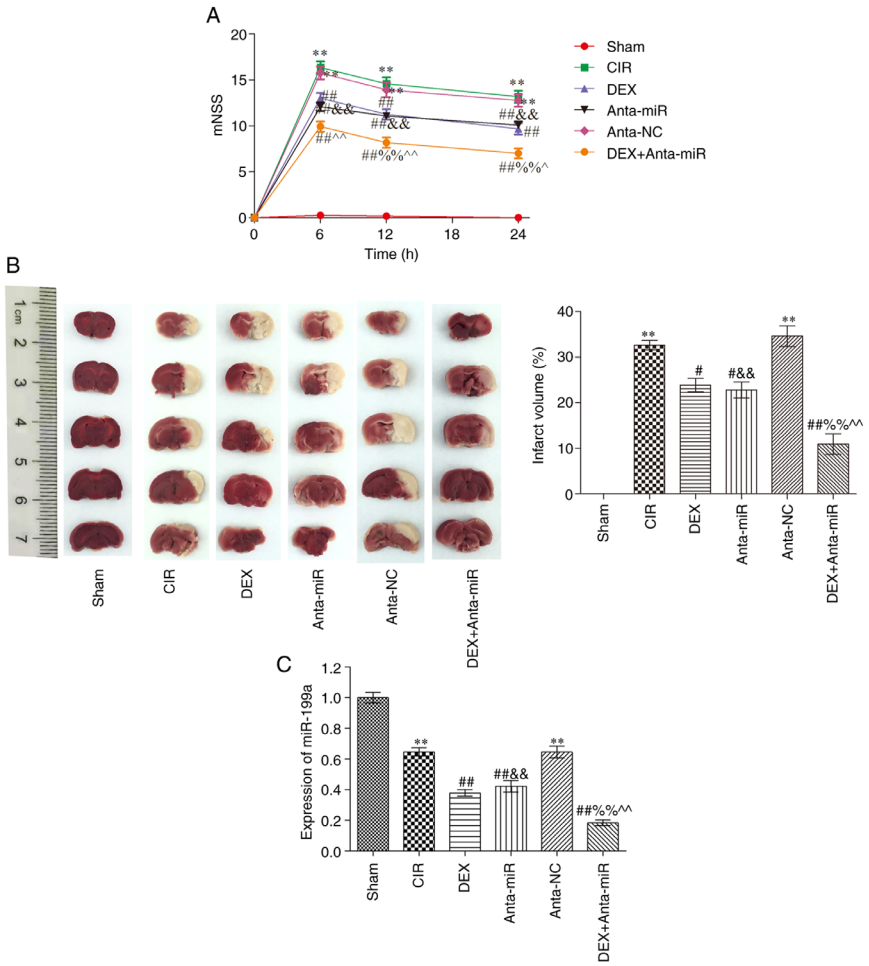

Figure 1. Effect of DEX on behavior of rats with CIR. (A) mNSS (n=12). (B) TTC staining of brain slices from one rat/group (n=6). (C) miR-199a expression was analyzed using reverse transcription-quantitative PCR (n=6). **P<0.01 vs. Sham; $^{\#}$P<0.05, $^{\#\#}$P<0.01 vs. CIR; $^{\&\&}$P<0.01 vs. anta-NC; $^{\wedge}$P<0.05, $^{\wedge\wedge}$P<0.01 vs. DEX; $^{\%\%}$P<0.01 vs. anta-miR. CIR, cerebral ischemia-reperfusion; DEX, dexmedetomidine; anta, antagomir; miR, microRNA; NC, negative control; mNSS, modified neurological severity score.

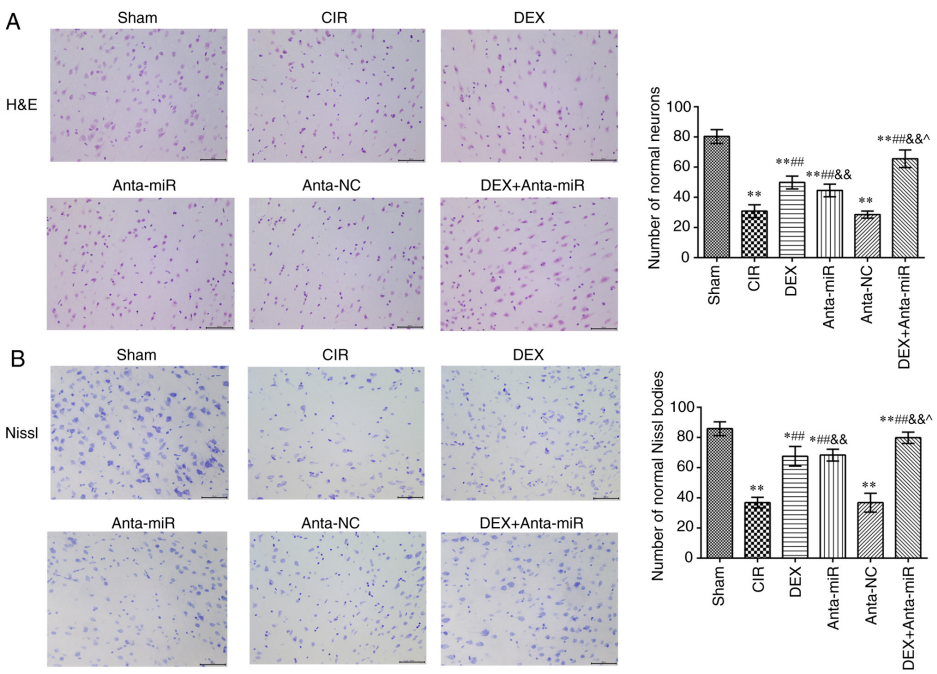

Figure 2. Effects of DEX on histopathology of the cerebral cortex in rats with CIR. (A) H&E staining. Scale, 50 μm. (B) Nissl staining. Scale, 50 μm. Magnification, x400 (n=6). *P<0.05, **P<0.01 vs. Sham; $^{\#\#}$P<0.01 vs. CIR; $^{\&\&}$P<0.01 vs. anta-NC; $^{\wedge}$P<0.05 vs. DEX. CIR, cerebral ischemia-reperfusion; DEX, dexmedetomidine; anta, antagomir; miR, microRNA; NC, negative control; H&E, hematoxylin and eosin.

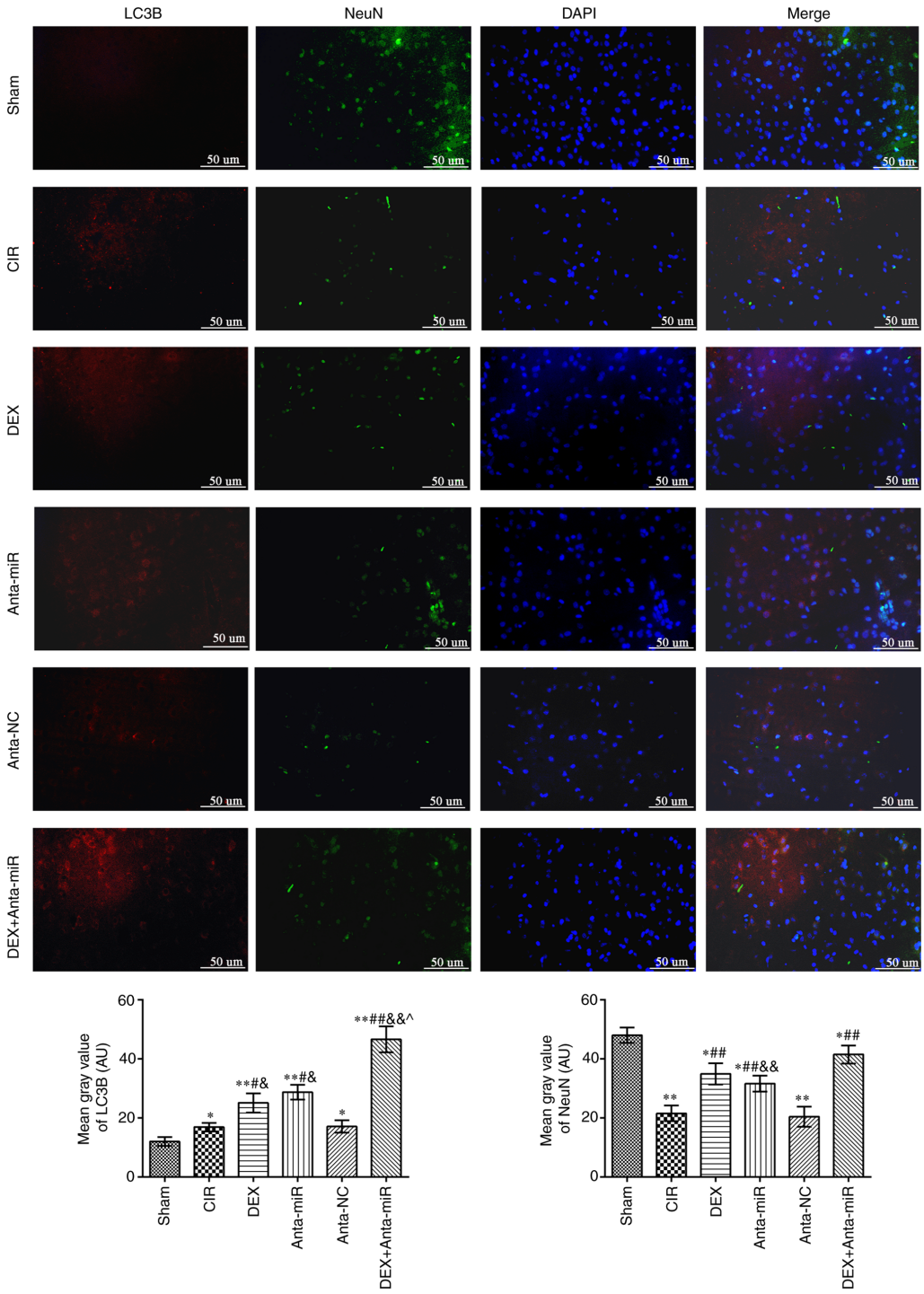

Figure 3. DEX induces co-localization of NeuN and LC3B in the cerebral cortex of rats with CIR. Immunofluorescence staining was used to detect co-expression of NeuN and LC3B. Scale bar, 50 μm. Magnification, x400 (n=6). *P<0.05, **P<0.01 vs. Sham; $^{\#}$P<0.05, $^{\#\#}$P<0.01 vs. CIR; $^{\&}$P<0.05, $^{\&\&}$P<0.01 vs. anta-NC; $^{\wedge}$P<0.05 vs. DEX. LC3B, microtubule-associated proteins 1A/1B light chain 3B; CIR, cerebral ischemia-reperfusion; DEX, dexmedetomidine; anta, antagomir; miR, microRNA; NC, negative control.

In the CIR and anta-NC groups, neuron and nucleolus loss and nuclear pyk-nosis were observed. Following DEX or anta-miR intervention, the loss of neurons and pyknosis decreased. Following co-treatment with DEX and anta-miR, pyknosis of the nucleus was weak, and almost no loss of neurons was observed. Nissl staining revealed that neurons in the Sham group contained abundant Nissl bodies with normal structure and clear integrity (Fig. 2B). In the CIR and anta-NC groups, the normal neuronal structure was destroyed, and the number of Nissl bodies was decreased. The number of Nissl bodies in the DEX and anta-miR groups was significantly higher than in the CIR group, and the number of Nissl bodies increased further after DEX was combined with anta-miR treatment. These results suggested that DEX improved the brain pathological injury by regulating miR-199a.

Effect of DEX on expression of LC3B in the cerebral cortex of rats with CIR. Fig. 3 shows fluorescence microscopy results

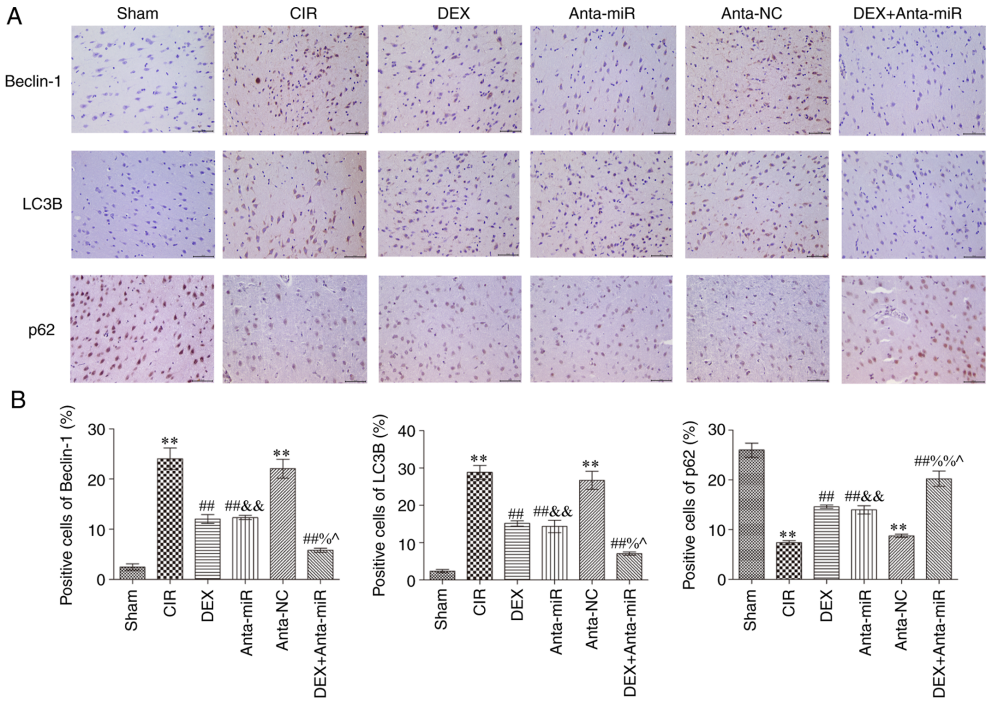

Figure 4. DEX inhibits expression of Beclin1, LC3B and p62 in the cerebral cortex of rats with CIR. (A) Immunohistochemical staining. Scale, 50 μm. (B) Quantitative analysis of Beclin1, LC3B and p62 levels. Magnification, x400 (n=6). **P<0.01 vs. Sham; $^{\#\#}$P<0.01 vs. CIR; $^{\&\&}$P<0.01 vs. anta-NC; $^{\wedge}$P<0.05 vs. DEX; $^{\%}$P<0.05, $^{\%\%}$P<0.01 vs. anta-miR. CIR, cerebral ischemia-reperfusion; LC3B, microtubule-associated proteins 1A/1B light chain 3B; DEX, dexmedetomidine; Anta, antagomir; miR, microRNA; NC, negative control.

of double staining with LC3B (red) and NeuN (green). The fluorescence intensity of LC3B in the cerebral cortex of the CIR and anta-NC groups was significantly higher than that of the Sham group, while the NeuN inten-sity decreased. The fluorescence intensity of LC3B and NeuN increased following DEX or anta-miR treatment compared with that of the CIR group. LC3B was primarily expressed in the cytoplasm, whereas NeuN was expressed in the nucleus. This indicated that the mechanism of DEX regulating miR-199a was associated with autophagy.

Effect of DEX on expression of autophagy-associated proteins in the cerebral cortex of rats with CIR. Immunohistochemical analysis of autophagy-associated proteins in the cerebral cortex revealed that expression of Beclin1 and LC3B in the CIR and anta-NC groups was significantly increased, while the expression of p62 was significantly decreased compared with the Sham group (Fig. 4). Following DEX and anta-miR inter-vention, Beclin1 and LC3B protein expression levels were significantly lower than those in the CIR group, while p62 protein expression significantly increased In addition, the expression levels of Beclin1 and LC3B decreased, while protein expression of p62 was increased following co-treatment with DEX and anta-miR. These data further demonstrated that DEX regulation of miR-199a in CIR was associated with autophagy.

Effects of DEX on expression of Beclin1, LC3B, p62 and cleaved caspase-3 in the cerebral cortex of rats with CIR. Western blot analysis showed that Beclin1, LC3B and cleaved caspase-3 protein expression levels were significantly increased in the CIR and anta-NC groups, while p62 protein expression was significantly decreased compared with the Sham group (Fig. 5). Compared with the CIR group, protein expression levels of p62 significantly increased following DEX and anta-miR intervention. In addition, the expression levels of Beclin1, LC3B and cleaved caspase-3 decreased, while those of p62 increased following co-treatment with DEX and anta-miR. These results were consistent with the results of the immunohistochemistry.

Discussion

Previous studies have shown that CIR causes oxidative stress, calcium regulation dis-order and autophagy (27-29). Autophagy is a common type of programmed cell death, which relies on the catabolism of autophagy lysosomes to degrade cytoplasmic content and recycle resources (30). Abnormal autophagy is associated with tumors, as well as neurodegenerative, metabolic and immune disease (31). LC3 is a marker of autophagy and is primarily involved in the formation of autophagy (32). The precursor molecule of LC3 is cleaved by autophagy-related 4B cysteine peptide to form the cytoplasmic form LC3-i. In mammals, there are four LC3 isoforms (LC3A, LC3B, LC3B2 and LC3C), and their expression varies in different tissue and cell types (33). In previous studies (32-34), LC3B has been demonstrated to be highly expressed in the brain and endocrine tissue, but not in liver, colon, myocardium or spleen. Beclin1, p62 and cleaved caspase-3 are associated with LC3B (33). The present study detected co-expression of LC3B and the neuron marker NeuN. It was found that DEX inhibited autophagy and decreased nerve cell injury.

Previous studies have found that DEX improves the survival rate of neurons following transient global or focal

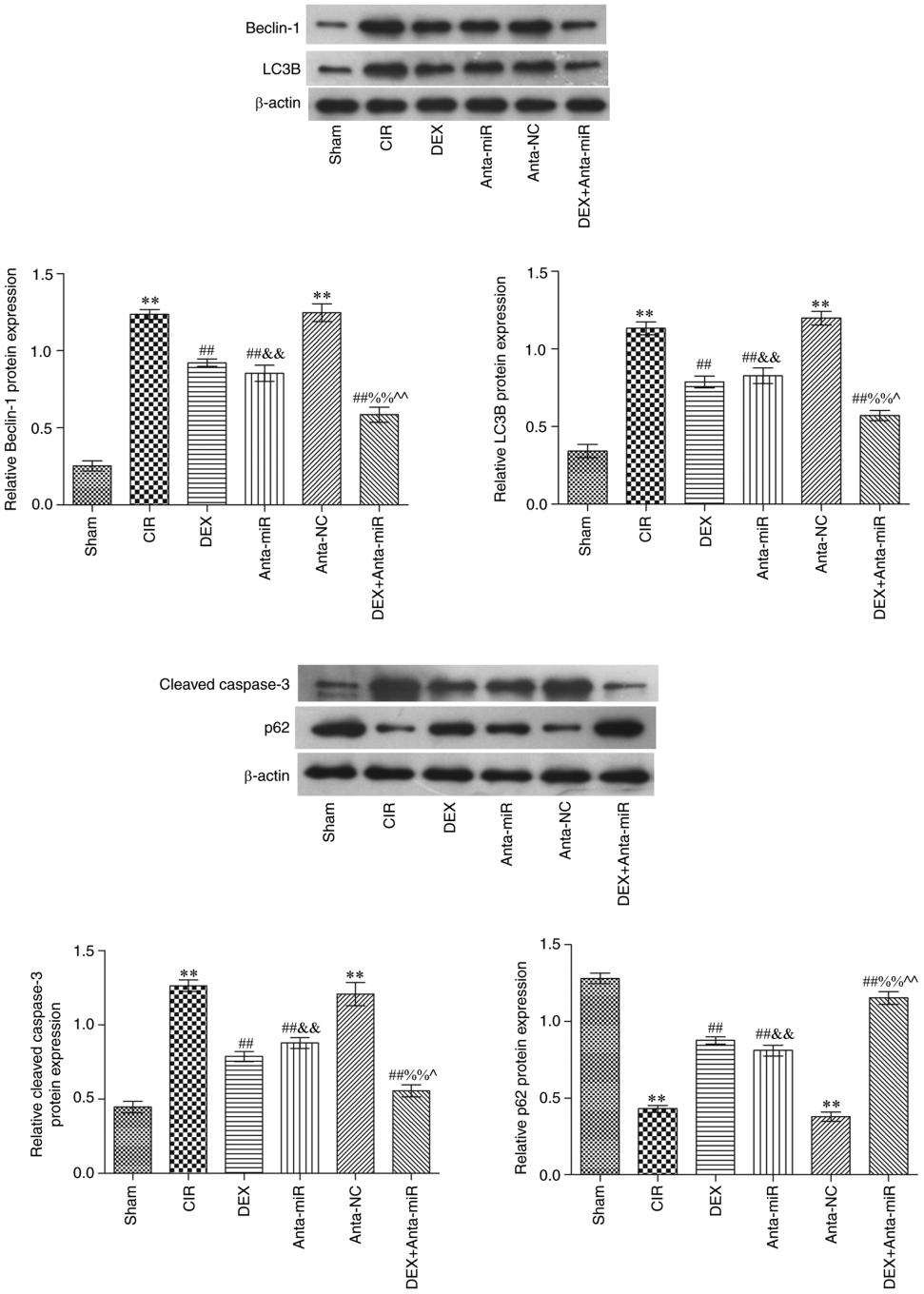

Figure 5. DEX inhibits expression of Beclin1, LC3B, p62 and cleaved caspase-3 in the cerebral cortex of rats with CIR. Relative protein expression levels in cerebral cortex (n=6). **P<0.01 vs. Sham; $^{\#\#}$P<0.01 vs. CIR; $^{\&\&}$P<0.01 vs. anta-NC; $^{\wedge}$P<0.05, $^{\wedge\wedge}$P<0.01 vs. DEX; $^{\%\%}$P<0.01 vs. anta-miR. CIR, cer-ebral ischemia-reperfusion; DEX, dexmedetomidine; anta, antagomir; miR, microRNA; NC, negative control; LC3B, microtubule-associated proteins 1A/1B light chain 3B.

cerebral ischemia in rats, and serves an important protective role in neuronal injury induced by cerebral ischemia by inhibiting activation of astrocytes (11,35). The present study found that DEX decreased mNSS and improved pathological damage of the cerebral cortex. A previous study also found that DEX protects PC12 cells from oxidative damage via regulation of miR-199a/hypoxia inducible factor 1α (36). Thus, the present study aimed to investigate the association between DEX and miR-199a in neuron injury. It was found that DEX inhibited the expression of miR-199a. A previous study found that DEX decreases glutamate agonist-induced neuronal apoptosis, which is associated with increased expression levels of brain-derived neurotrophic factor in astrocytes (37). To the best of our knowledge, however, the association between DEX and autophagy in CIR has not been reported, and the mechanism of DEX *in vitro* needs further investigation.

There is limited research on the temporal changes of miRNAs in cerebral ischemic tolerance (38). It has been reported that 24 h after ischemic preconditioning, the expression of miRNA in the cortex of adult mice changes (38,39). miR-199a shows similar temporal changes in cerebral cortex

and striatum, and overexpression of miR-199a decreases brain microvascular endothelial cell (BMEC) death, inflammation and angiogenesis (40). These results confirm that miR-199a has a protective effect on BMECs by inhibiting the pathophysiological process during and after oxygen-glucose deprivation and reperfusion. This provides a novel insight for understanding the molecular mecha-nism of microvascular injury, blood-brain barrier dysfunction and inflammation follow-ing ischemic stroke, which is important for improving the treatment of ischemic stroke (40,41). The present study found that DEX and anta-miR pretreatment decreased levels of miR-199a. Therefore, the present results showed that DEX protected against CIR injury by targeting miR-199a. This finding may serve as a guide for the treatment of patients with stroke. However, the mechanism of DEX and miR-199a in cerebral ischemia remains unclear. Further *in vitro* studies with specific cells or co-cultured cells are needed to improve understanding of the potential mechanisms and to identify prom-ising therapeutic targets.

In conclusion, DEX inhibited miR-199a, activated autophagy and alleviated injury of nerve cells induced by CIR in rats.

Acknowledgements

Not applicable.

Funding

No funding was received.

Availability of data and materials

The datasets used and/or analyzed during the current study are available from the corre-sponding author on reasonable request.

Authors' contributions

YL conceptualized and designed the study and software. YZ and YL curated the data, performed the experiments and wrote the manuscript. HZ and XM visualized the data, performed the experiments and supervised the study. WZ contributed the study design, wrote, reviewed and edited the manuscript. YL and HZ confirmed the authenticity of all the raw data. All authors read and approved the final manuscript.

Ethics approval and consent to participate

The present study was approved by the Animal Protection and Use Committee of Yan-taishan Hospital (Yantai, China; approval no. 2020-15).

Patient consent for publication

Not application.

Competing interests

The authors declare that they have no competing interests.

References

1. Paul S and Candelario-Jalil E: Emerging neuroprotective strategies for the treatment of ischemic stroke: An overview of clinical and preclinical studies. Exp Neurol 335: 113518, 2021.
2. Barteczek P, Li L, Ernst AS, Böhler LI, Marti HH and Kunze R: Neuronal HIF-1α and HIF-2α deficiency improves neuronal survival and sensorimotor function in the early acute phase after ischemic stroke. J Cereb Blood Flow Metab 37: 291-306, 2017.
3. Choi JI, Ha SK, Lim DJ, Kim SD and Kim SH: S100ß, matrix metalloproteinase-9, D-dimer, and heat shock protein 70 are serologic biomarkers of acute cerebral infarction in a mouse model of transient MCA occlusion. J Korean Neurosurg Soc 61: 548-558, 2018.
4. Doherty J and Baehrecke EH: Life, death and autophagy. Nat Cell Biol 20: 1110-1117, 2018.
5. Carloni S, Albertini MC, Galluzzi L, Buonocore G, Proietti F and Balduini W: Melatonin reduces endoplasmic reticulum stress and preserves sirtuin 1 expression in neuronal cells of newborn rats after hypoxia-ischemia. J Pineal Res 57: 192-199, 2014.
6. Zhang W and Zhang J: Dexmedetomidine preconditioning protects against lung inju-ry induced by ischemia-reperfusion through inhibition of autophagy. Exp Ther Med 14: 973-980, 2017.
7. Zhang W, Zhang JQ, Meng FM and Xue FS: Dexmedetomidine protects against lung ischemia-reperfusion injury by the PI3K/Akt/HIF-1α signaling pathway. J Anesth 30: 826-833, 2016.
8. Wang YQ, Tang YF, Yang MK and Huang XZ: Dexmedetomidine alleviates cerebral ischemia-reperfusion injury in rats via inhibition of hypoxia-inducible factor-1α. J Cell Biochem: Nov 19, 2018 (Epub ahead of print). doi: 10.1002/jcb.28058.
9. Begum G, Yan HQ, Li L, Singh A, Dixon CE and Sun D: Docosahexaenoic acid reduces ER stress and abnormal protein accumulation and improves neuronal function following traumatic brain injury. J Neurosci 34: 3743-3755, 2014.
10. Hetta DF, Kamal EE, Mahran AM, Ahmed DG, Elawamy A and Abdelraouf AM: Efficacy of local dexmedetomidine add-on for spermatic cord block anesthesia in patients undergoing intra-scrotal surgeries: Randomized controlled multicenter clinical trial. J Pain Res 10: 2621-2628, 2017.
11. Liu C, Fu Q, Mu R, Wang F, Zhou C, Zhang L, Yu B, Zhang Y, Fang T and Tian F: Dexmedetomidine alleviates cerebral ischemia-reperfusion injury by inhibiting endoplasmic reticulum stress dependent apoptosis through the PERK-CHOP-Caspase-11 pathway. Brain Res 1701: 246-254, 2018.
12. Guo H, Ingolia NT, Weissman JS and Bartel DP: Mammalian microRNAs predom-inantly act to decrease target mRNA levels. Nature 466: 835-840, 2010.
13. Guo D, Ma J, Yan L, Li T, Li Z, Han X and Shui S: Down-regulation of lncrna MALAT1 attenuates neuronal cell death through suppressing beclin1-dependent autophagy by regulating mir-30a in cerebral ischemic stroke. Cell Physiol Biochem 43: 182-194, 2017.
14. Wu P, Zuo X, Deng H, Liu X, Liu L and Ji A: Roles of long noncoding RNAs in brain development, functional diversification and neurodegenerative diseases. Brain Res Bull 97: 69-80, 2013.
15. Zhang J, Yuan L, Zhang X, Hamblin MH, Zhu T, Meng F, Li Y, Chen YE and Yin KJ: Altered long non-coding RNA transcriptomic profiles in brain microvascular endothelium after cerebral ischemia. Exp Neurol 277: 162-170, 2016.
16. Ebert MS and Sharp PA: Roles for microRNAs in conferring robustness to biolog-ical processes. Cell 149: 515-524, 2012.
17. Yu J, Wang F, Yang GH, Wang FL, Ma YN, Du ZW and Zhang JW: Human microRNA clusters: Genomic organization and expression profile in leukemia cell lines. Biochem Biophys Res Commun 349: 59-68, 2006.
18. Calame K: MicroRNA-155 function in B Cells. Immunity 27: 825-827, 2007.
19. Yao S, Tang B, Li G, Fan R and Cao F: miR-455 inhibits neuronal cell death by targeting TRAF3 in cerebral ischemic stroke. Neuropsychiatr Dis Treat 12: 3083-3092, 2016.
20. Yin KJ, Deng Z, Huang H, Hamblin M, Xie C, Zhang J and Chen YE: miR-497 regulates neuronal death in mouse brain after transient focal cerebral ischemia. Neurobiol Dis 38: 17-26, 2010.
21. National Research Council (US) Committee for the Update of the Guide for the Care and Use of Laboratory Animals: Guide for the Care and Use of Laboratory Animals. 8th edition. National Academies Press (US), Washington, DC, pp963-965, 2011.
22. Longa EZ, Weinstein PR, Carlson S and Cummins R: Reversible middle cerebral artery occlusion without craniectomy in rats. Stroke 20: 84-91, 1989.

23. Sha R, Han X, Zheng C, Peng J, Wang L, Chen L and Huang X: The effects of electroacupuncture in a rat model of cerebral ischemia-reperfusion injury following middle cerebral artery occlusion involves microRNA-223 and the PTEN signaling pathway. Med Sci Monit 25: 10077-10088, 2019.
24. Wang D, Li Z, Zhang Y, Wang G, Wei M, Hu Y, Ma S, Jiang Y, Che N, Wang X, *et al*: Targeting of microRNA-199a-5p protects against pilocarpine-induced status epilepticus and seizure damage via SIRT1-p53 cascade. Epilepsia 57: 706-716, 2016.
25. Chen J, Sanberg PR, Li Y, Wang L, Lu M, Willing AE, Sanchez-Ramos J and Chopp M: Intravenous administration of human umbilical cord blood reduces behavioral deficits after stroke in rats. Stroke 32: 2682-2688, 2001.
26. Livak KJ and Schmittgen TD: Analysis of relative gene expression data using real-time quantitative PCR and the 2(-Delta Delta C(T)) Method. Methods 25: 402-408, 2001.
27. Hei C, Liu P, Yang X, Niu J and Li PA: Inhibition of mTOR signaling confers protection against cerebral ischemic injury in acute hyperglycemic rats. Int J Biol Sci 13: 878-887, 2017.
28. Jiang M, Li J, Peng Q, Liu Y, Liu W, Luo C, Peng J, Li J, Yung KK and Mo Z: Neuroprotective effects of bilobalide on cerebral ischemia and reperfusion injury are associated with inhibition of pro-inflammatory mediator production and down-regulation of JNK1/2 and p38 MAPK activation. J Neuroinflammation 11: 167, 2014.
29. Halestrap AP: Calcium, mitochondria and reperfusion injury: A pore way to die. Biochem Soc Trans 34: 232-237, 2006.
30. Carloni S, Girelli S, Scopa C, Buonocore G, Longini M and Balduini W: Activation of autophagy and Akt/CREB signaling play an equivalent role in the neuroprotective effect of rapamycin in neonatal hypoxia-ischemia. Autophagy 6: 366-377, 2010.
31. Chu CT: Mechanisms of selective autophagy and mitophagy: Implications for neurodegenerative diseases. Neurobiol Dis 122: 23-34, 2019.
32. Descloux C, Ginet V, Clarke PG, Puyal J and Truttmann AC: Neuronal death after perinatal cerebral hypoxia-ischemia: Focus on autophagy-mediated cell death. Int J Dev Neurosci 45: 75-85, 2015.
33. Qian X, Li X, Cai Q, Zhang C, Yu Q, Jiang Y, Lee JH, Hawke D, Wang Y, Xia Y, *et al*: Phosphoglycerate kinase 1 phosphorylates beclin1 to induce autophagy. Mol Cell 65: 917-931.e6, 2017.
34. Huang L, Chen C, Zhang X, Li X, Chen Z, Yang C, Liang X, Zhu G and Xu Z: Neuroprotective Effect of Curcumin against cerebral ischemia-reperfusion via mediating autophagy and inflammation. J Mol Neurosci 64: 129-139, 2018.
35. Aryan HE, Box KW, Ibrahim D, Desiraju U and Ames CP: Safety and efficacy of dexmedetomidine in neurosurgical patients. Brain Inj 20: 791-798, 2006.
36. Wu L, Xi Y and Kong Q: Dexmedetomidine protects PC12 cells from oxidative damage through regulation of miR-199a/HIF-1α. Artif Cells Nanomed Biotechnol 48: 506-514, 2020.
37. Yin D, Zhou S, Xu X, Gao W, Li F, Ma Y, Sun D, Wu Y, Guo Q, Liu H, *et al*: Dexmedetomidine attenuated early brain injury in rats with subarachnoid haemorrhage by suppressing the inflammatory response: The TLR4/NF-κB pathway and the NLRP3 inflammasome may be involved in the mechanism. Brain Res 1698: 1-10, 2018.
38. Wang P, Liang J, Li Y, Li J, Yang X, Zhang X, Han S, Li S and Li J: Down-regulation of miRNA-30a alleviates cerebral ischemic injury through enhancing beclin 1-mediated autophagy. Neurochem Res 39: 1279-1291, 2014.
39. Rane S, He M, Sayed D, Vashistha H, Malhotra A, Sadoshima J, Vatner DE, Vat-ner SF and Abdellatif M: Downregulation of miR-199a derepresses hypoxia-inducible factor-1alpha and Sirtuin 1 and recapitulates hypoxia preconditioning in cardiac myocytes. Circ Res 104: 879-886, 2009.
40. Zuo Y, Wang Y, Hu H and Cui W: Atorvastatin protects myocardium against ischemia-reperfusion injury through inhibiting miR-199a-5p. Cell Physiol Biochem 39: 1021-1030, 2016.
41. Xu WH, Yao XY, Yu HJ, Huang JW and Cui LY: Downregulation of miR-199a may play a role in 3-nitropropionic acid induced ischemic tolerance in rat brain. Brain Res 1429: 116-123, 2012.